Coastal-trapped Wave Scattering into and out of Straits and Bays

JOHN F. MIDDLETON

School of Mathematics, University of New South Wales, Kensington, N.S.W., Australia

(Manuscript received 20 August 1990, in final form 22 October 1990)

ABSTRACT

A theory for the generation of coastal-trapped waves (CTWs) by an oscillatory coastal flux through a strait is extended so as to make velocity, pressure and energy flux everywhere continuous. This development is achieved through the inclusion of Kelvin and Poincaré wave modes in a match for pressure leading to a system of linear equations for the unknown amplitudes. A Kelvin wave incident on the eastern mouth of Bass Strait for example is shown to preferentially scatter energy into CTW modes 2 and 1 on the shelf, as well as driving a Poincaré wave field that results in a velocity jet trapped to the Victorian coast. Such coastal velocity jets are also a feature of the scattering of CTWs incident on a strait. For a mode n incident CTW, the fraction of net energy flux that enters the strait is also shown to be well approximated by $h_0 b_n^2$ where h_0 is the strait depth and b_n a coupling coefficient. The scattering of the remaining energy among other CTW modes is detailed and shown to become larger as the incident mode number or frequency is increased. Similar results are also found for the scattering by a bay and while the net energy flux into a bay will in general be near zero, the coastal jets on each side of the bay may significantly effect the local circulation.

1. Introduction

In recent years considerable progress has been made in understanding how coastal-trapped waves (CTWs) may be generated and scattered by straits and bays. In a barotropic analysis, Buchwald and Kachoyan (1987) have detailed the shelf wave response to forcing by a prescribed oscillatory coastal flux through Bass Strait. This analysis while valid at all subinertial frequencies is restricted to an exponential shelf topography and allows for both long and short wave modes. The results obtained did suggest however that the response on the east Australian shelf should be dominated by modes 2 and 1 as observed during the Australian Coastal Experiment (Church et al. 1986). The importance of an oscillatory coastal flux in driving CTWs has also been demonstrated for the Hudson Strait/Labrador Shelf region by Wright et al. (1987). In this barotropic analysis a step-shelf was assumed and only mode 1 and the Kelvin wave were generated, although the results were successful in predicting the coastal response of adjusted sea level some 500 km south of the strait. For the idealized topography assumed, Wright et al. (1987) also detailed how the energy of a mode 1 shelf wave may be scattered into Hudson Strait and Bay and subsequently rescattered onto the Labrador Shelf. An additional feature of this work was in showing how large bays may be resonantly forced by atmospheric pressure variations resulting in the coastal forcing of shelf waves.

Corresponding author address: Dr. John F. Middleton, School of Mathematics, University of New South Wales, P.O. Box 1, Kensington, New South Wales, Australia, 2033.

The scattering of shelf wave energy by rectangular bays has also been addressed by Stocker and Johnson (1989). In their barotropic analysis, exponential profiles of both the shelf and bay/shelf regions were assumed and the scattering of incident energy into short waves and standing trapped waves was detailed. Both this and the barotropic analysis of Buchwald and Kachoyan (1987) assume the existence of short waves, although such waves may not exist at low frequencies in stratified seas (Chapman 1983) or in regions where a mean alongshore current exists (Webster and Narayanan 1988).

A scattering theory, which does not rely on the existence short waves, has been advanced by Middleton (1988) who showed that the forcing of long CTWs by an oscillatory coastal flux is directly analogous to forcing by wind stress. Middleton (1988) was able to demonstrate that the CTW response to a coastal flux may be obtained for arbitrary shelf bathymetries in frictional, stratified seas using existing theories for wind-forced CTWs. This analysis was however restricted to low frequencies where the long-wave approximation is valid, and as with the work of Buchwald and Kachoyan (1987), the coastal velocity flux was prescribed and no account was taken of the dynamics of the strait or if pressure was continuous across the strait mouth.

Most recently Middleton and Viera (1991) have examined sea level and current meter data from Bass Strait (Fig. 1a) to show that local wind and CTWs incident from the Great Australian Bight, are of equal importance in driving an oscillatory flux through the eastern strait mouth, at a period of 240 h. The models for forcing developed by Middleton and Viera (1991)

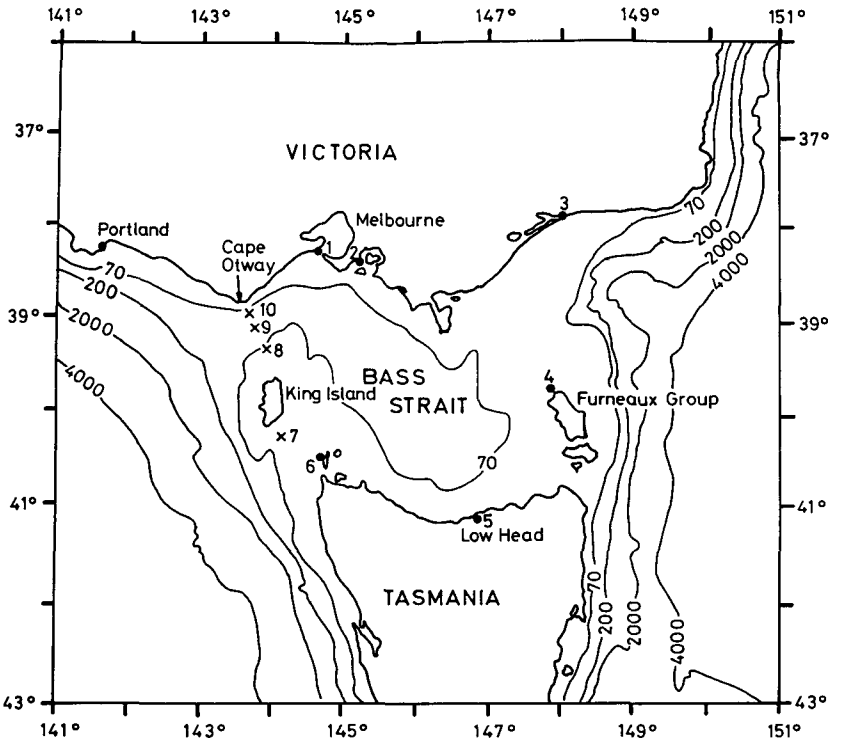

FIG. 1a. The bathymetry of the Bass Strait region where depths are in meters and the solid circles and crosses denote the site positions of sea level and current meter data that were analyzed by Middleton and Viera (1991).

allowed for scattering of CTW energy into and out of the strait by directly matching coastal sea level within the strait (dominated by forced Kelvin waves) to sea level on the adjacent shelves (dominated by the CTWs there incident or generated). This analysis, while reasonably successful in predicting the variability of coastal sea level within Bass Strait, was unable to adequately describe the observations of current near the western strait mouth. As we will see, this inadequacy arises in part from the models developed, where pressure was not matched at all points across the regions separating the strait and adjacent shelves.

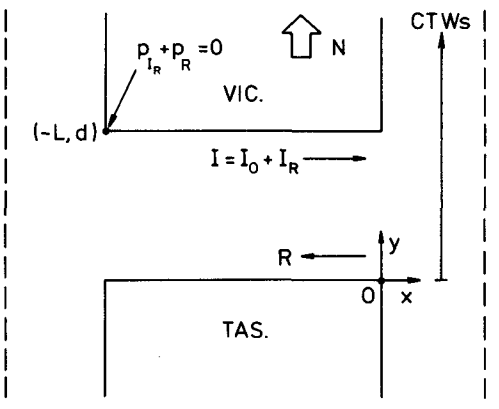

FIG. 1b. The idealized bathymetry of Bass Strait of length $L = 416$ km, width $d = 230$ km, and depth $h_0 = 70$ m. Incident (I) and reflected (R) Kelvin waves are indicated along with the direction of CTW propagation. Note that the incident wave may be regarded as consisting of two components I_0 and I_R where the former corresponds to, say, a wave generated within the strait, and the latter to a wave that is reflected at the western strait mouth for which $p_R + p_{I_R} \approx 0$ at $\mathbf{x} = (-L, d)$.

In the analysis below, the scattering theories of Middleton (1988) and Middleton and Viera (1991) are extended so as to allow for continuity of velocity and pressure across the strait mouths. In section 2, the theory for the generation of CTWs by a coastal flux is outlined through the inclusion of the Kelvin waves and the Poincaré waves that may be supported within a strait. For illustrative purposes we will consider (section 3) the case of Bass Strait, while in section 4 the problem of scattering of CTW energy into the strait and also a rectangular bay is addressed. Since we are here concerned with elucidating the physics and solution techniques for these problems, only the generation of long barotropic waves is examined, although as will become evident, the analysis may be extended to the scattering of CTWs in a stratified ocean. For this reason long barotropic shelf waves will be referred to as CTWs.

2. Scattering out of a strait: Theory

The governing equations for barotropic, linear motions in a frictional sea may be written as

$$u_t - fv = -p_x/\rho - ru/h \tag{2.1a}$$

$$v_t + fu = -p_y/\rho - rv/h \tag{2.1b}$$

$$p_t + \rho g \nabla \cdot (h\mathbf{u}) = 0, \tag{2.1c}$$

where the (x, y) coordinate system is defined in Fig. 1b and $f = -9.15 \times 10^{-5}$ sec^{-1} denotes the Coriolis parameter for the Bass Strait region. Within the strait the depth h is taken as the constant $h_0 = 70$ m while on the shelf $h = h(x)$. Bottom friction is incorporated through the parameter r and in the following (u, v, p) are assumed to be proportional to $\exp(-i\omega t)$, where frequency ω is positive.

At low frequencies, where terms of order $(\omega/f)^2$ may be neglected, the equations for the strait may be combined to yield

$$\nabla^2 p - \alpha^2 p = 0, \tag{2.2}$$

where

$$\alpha^{-1} = \mathrm{sgn}(f)\theta\sqrt{gh_0}/|f| \tag{2.3}$$

denotes the deformation radius modified by the effects of friction through

$$\theta = \mathrm{sgn}(f)(1 + ir/\omega h_0)^{1/2}. \tag{2.4}$$

Now, consider a Kelvin wave that is incident on the eastern edge of the idealized strait (width d) as shown in Fig. 1b. As a solution to (2.2) it may be written as

$$p_I = Ie^{\alpha y}\exp(-il_0 x), \tag{2.5}$$

where I denotes a specified amplitude and $l_0 = \omega\theta/\sqrt{gh_0}$ the wavenumber, assuming that $|l_0| \ll |\alpha|$ and $v \equiv 0$ on the Victorian and Tasmanian coastal boundaries. Note that for Bass Strait f is negative so that the incident wave propagates with the coast on its left as shown in Fig. 1b. This wave will also scatter energy onto the shelf as well as into a reflected wave

$$p_R = Re^{-\alpha y}\exp(il_0 x), \tag{2.6}$$

where the coefficient R is to be determined. In addition, we may expect a Poincaré wave field to be generated near the inner edge of the strait. At the low frequencies of interest these waves are evanescent in the x direction and from (2.2) the nth mode may be derived as

$$p_n(x, y) = \sin(r_n y + \epsilon)e^{r_n x}, \quad x \leq 0, \tag{2.7}$$

where $r_n = n\pi/d$ and $\epsilon = -i\omega\theta^2/f$. Terms of order $(\omega/f)^2$ and $(\alpha/r_n)^2$ have been neglected and for Bass Strait, $|\alpha^{-1}| \sim 306$ km and $d = 230$ km, so that $|\alpha/r_n|^2 \sim (n\pi)^{-2} \ll 1$. Note that the Poincaré wave contribution to coastal pressure is from (2.7) of order $\epsilon \sim |\omega/f|$. For Bass Strait the energy containing band has been identified as that corresponding to 240 h (Middleton and Viera, 1991) so that $\epsilon \sim 0.08$ and the Poincaré wave contribution to coastal pressure is small. The velocity field associated with the Poincaré waves is given by

$$\left.\begin{aligned} v_n &= (\rho f)^{-1} r_n \sin(r_n y)e^{r_n x} \\ u_n &= -(\rho f)^{-1} r_n \cos(r_n y)e^{r_n x} \end{aligned}\right\} \tag{2.8}$$

if again terms of order $(\omega/f)^2$ and $(\alpha/r_n)^2$ are neglected.

Within the strait, the solution for the scattering of the incident wave p_I will be assumed to consist of the reflected wave (2.6) and the Poincaré waves (2.7), so that at $x = 0^-$

$$p(0^-, y) = Ie^{\alpha y} + Re^{-\alpha y} + \sum_1^\infty d_n \sin(r_n y + \epsilon), \tag{2.9}$$

where the d_n denote amplitudes to be determined. The net time-averaged energy flux through the strait (subscript $_{st}$) is given by

$$\Gamma_{st} = \tfrac{1}{4} h_0 \int_0^d [u^* p + u p^*]\, dy, \tag{2.10}$$

where the asterisk denotes the complex conjugate. It may be shown that the evanescent Poincaré waves make no contribution to Γ_{st} and since the Kelvin wave velocity u is in geostrophic balance, (2.10) may be written as

$$\Gamma_{st} = -(h_0/4\rho f)[p_K p_K^*]_0^d, \tag{2.11}$$

where p_K is the pressure due to the Kelvin waves alone.

The incident Kelvin wave will also act to generate CTWs on the shelf through the displacement of fluid columns into deeper or shallower water. Such CTW generation by a prescribed oscillatory velocity field at a strait mouth has been examined by Middleton (1988). The basis of the technique is to expand the velocity field at the strait mouth,

$$U(y) \equiv u(0^-, y) = u(0^+, y) \tag{2.12}$$

in terms of the eigenfunctions for CTW pressure $F_n(x)$, where for the nth mode

$$p_n(x, y) = F_n(x)\phi_n(y)$$

and the $\phi_n(y)$ satisfy the forced long-wave equation

$$(-i\omega/c_n)\phi_n + \phi_{ny} + r\sum_{m=0}^{\infty} a_{nm}\phi_m = -\rho f h_0 b_n U(y), \tag{2.13}$$

where $c_n = \omega/k_n$ is the phase speed,

$$b_n = F_n(0) \tag{2.14}$$

a coupling coefficient such that

$$h_0 \sum b_n^2 = 1 \tag{2.15}$$

and the a_{nm} an infinite set of frictional damping coefficients, (Brink 1982; Clarke and Van Gorder 1986). For readers unfamiliar with the analysis of Middleton (1988), the wave equation (2.13) for forcing by a coastal flux is directly analogous to that of forcing by

an alongshore component of wind stress τ since if we identify $U = -\tau/\rho f h_0$, the velocity U then simply corresponds to the Ekman velocity at the coast that is driven by the wind.

For illustrative purposes, we shall adopt a simpler model for friction than that given in (2.13) and truncate the sum to $a_{nn}\phi_n$ so that $a_{nm} = 0$ for $m \neq n$. In this case (2.13) may be integrated immediately to obtain

$$\phi_n(y) = -\rho f h_0 b_n \int_0^y U(\zeta) e^{-iK_n(\zeta - y)} d\zeta \quad (2.16)$$

for $0 \leqslant y \leqslant d$, where $K_n = k_n + \gamma_n i$ and $\gamma_n = r a_{nn}$. The eigenfunctions F_n, b_n, K_n, etc., are all readily calculated from the suite of CTW programs of Brink and Chapman (1985), and using their normalization for the eigenfunctions, the net energy flux crossing the cross-shelf section at $y = d$ is given by

$$\Gamma_n = -\phi_n(d)\phi_n^*(d)/4\rho f. \quad (2.17)$$

Note that for $y \geqslant d$ the CTWs propagate as the free waves

$$p_n(x, y) = \phi_n(d) F_n(x) e^{iK_n(y-d)}. \quad (2.18)$$

For $0 \leqslant y \leqslant d$, the total CTW pressure field at $x = 0^+$ may now be written as

$$p(0^+, y) = -\rho f \int_0^y U(\zeta) G(\zeta - y) d\zeta, \quad (2.19)$$

where

$$G(\zeta) = h_0 \sum_{n=0}^{\infty} b_n^2 e^{-iK_n\zeta}. \quad (2.20)$$

The velocity field $U(y)$ at the strait mouth is by the definition (2.12) equal to that on either side of the strait mouth. Thus from the assumed Kelvin and Poincaré wave expansion within the strait, it is given by

$$-\rho f U(y) = \alpha\{Ie^{\alpha y} - Re^{-\alpha y}\} + \sum_1^{\infty} d_m r_m \cos(r_m y). \quad (2.21)$$

As (2.21) stands, $U(y)$ is not prescribed since the coefficients R and d_m are unknown. Indeed, their determination will result from the condition that pressure match across the strait mouth which from (2.9), (2.19) and (2.21) may be written as

$$Ie^{\alpha y} + Re^{-\alpha y} + \sum_1^{\infty} d_m \sin(r_m y + \epsilon) = \alpha \int_0^y \left\{ Ie^{\alpha\zeta} - Re^{-\alpha\zeta} + \frac{1}{\alpha} \sum_1^{\infty} d_m r_m \cos(r_m \zeta) \right\} \times G(\zeta - y) d\zeta = 0. \quad (2.22)$$

Solutions for R and the first N Poincaré wave amplitudes are to be obtained below from a matrix equation that results by (i) truncating the sum in (2.22) to N Poincaré modes and (ii) by evaluating (2.22) at the $N + 1$ points $y_i/d = i/(N + 2)$ for $i = 1, N + 1$; the Collocation Method, (Brown, 1973). The $N + 1$ linear equations in $N + 1$ unknowns may then be solved. A finite number of (eleven) CTW modes will also be assumed in the expression (2.20) for G. With the R and d_m determined, the strait and shelf pressure and velocity fields may then be constructed.

It should be noted that the above solution technique is formally only valid at low frequencies $(\omega/f)^2 \ll 1$, where the long-wave approximation is valid, and where the strait width d is of order or less than the deformation radius $\sqrt{gh_0}/|f|$; the latter condition follows from the assumption that $|\alpha/r_n|^2 \ll 1$. However, no restrictions are made on the shelf topography $h(x)$ and the analysis may be immediately extended to forcing of CTWs in a stratified ocean, (Middleton 1988). Quite simply, if the eigenfunctions $F_n(x, z)$ of the dominant modes generated in a stratified ocean are reasonably independent of depth z near the coast, then $F_n(x)$ in the above may simply be replaced by $F_n(x, z)$.

Finally, before presenting detailed solutions three points may be made about the above analysis. The first point is that the generated CTW pressure field (2.19) vanishes at $y = 0$ and since energy can only propagate forward of this site, $y = 0$ may be regarded as a "geographical origin". The second point is that at very low frequencies where $\epsilon \sim |\omega/f|$ is near zero, the coastal pressure within the strait is dominated by the Kelvin waves. Thus, from (2.9) the reflection coefficient may be immediately determined as

$$R = -I. \quad (2.23)$$

The final point to be made concerns the generation of the CTW modes. If we consider the simplistic case where the velocity flux is prescribed to be uniform $U = U_0$, then following Middleton (1988), (2.17) reduces to $\Gamma_n = -\frac{1}{4}\rho f(h_0 d b_n U_0)^2 \operatorname{sinc}^2(k_n d/2)$ in the inviscid limit. Now if the velocity U_0 within the strait is also in geostrophic balance, then the flux (2.11) out of the strait may be written as $\Gamma_{st} = -\frac{1}{4}\rho f h_0 d^2 U_0^2$ so that

$$\Gamma_n/\Gamma_{st} = h_0 b_n^2 \operatorname{sinc}^2(k_n d/2). \quad (2.24)$$

The point here is that the modes which will be most preferentially generated will be those for which $h_0 b_n^2$ is largest, i.e. those modes with the largest coupling coefficient b_n. As will be seen b_n may be largest for mode 2 rather than mode 1. The result (2.24) is as best approximate since as will be shown the flux U cannot be prescribed and may be far from uniform.

3. Scattering out of a strait: Results

In order to illustrate the scattering theory a shelf bathymetry was chosen that is typical of both the western and eastern sides of Bass Strait. The first 11 long-

TABLE 1. The long-wave phase speeds c_n, friction coupling coefficients a_{nn} and "wind" coupling coefficient b_n, expressed as $h_0 b_n^2$ where $h_0 = 70$ m. The latter form is chosen as it is a measure of the energy scattered into a strait (4.8) and out of a strait, (2.24).

CTW mode	c_n (m s^{-1})	$a_{nn} \times 10^3$ (s m^{-2})	$h_0 b_n^2 \times 10^2$
0	40.86	0.002	1.3243
1	3.23	0.596	19.4986
2	1.70	3.509	50.2505
3	0.84	2.228	8.0194
4	0.43	4.500	4.7983
5	0.29	7.176	4.2808
6	0.19	8.099	2.6049
7	0.15	29.240	8.8666
8	0.13	3.348	0.2933
9	0.10	2.907	0.0030
10	0.07	3.495	0.0004

wave eigenfunctions were then computed along with the c_n, a_{nn} and b_n, (Table 1). A friction parameter $r = 4.6 \times 10^{-4}$ m s^{-1} was chosen as typifying both friction within the strait (Clarke 1987) and very crudely, friction on the shelf resulting in a decay scale γ_n^{-1} that was at least $3k_n^{-1}$ (for modes 2 and 7) and generally more, $\gamma_n^{-1} \geq 6k_n^{-1}$ at the period of 240 h (10 days) assumed. The friction parameter chosen for the shelf is perhaps unrealistically large since the tidal velocities upon which it is based will be much weaker on the shelf than in the strait. However, since the model for friction is itself only approximate and as results for $r = 0$ will also be presented, we shall ignore this deficiency in this illustrative analysis.

The validity of the CTW modes at the frequencies of interest was also examined by determining the phase speeds c_1, c_2 and c_3 without resort to the long-wave approximation. In particular, these c_1, c_2 and c_3 were found to be 20% less than their long-wave counterparts in Table 1 at periods of 7.3, 5.9 and 14.4 days, respectively. Thus, even if all scattered energy resides in these and the Kelvin wave modes, the results below will not be formally valid for periods shorter than the 240 h or 10 days assumed here.

The scaled amplitudes d_m/I and R/I were obtained from (2.22) using the Collocation Method for $N = 11$ Poincaré modes. The results both with and without friction ($r = 0$) are presented in Table 2 and show that the $|d_m|$ decrease rapidly with m: $|d_{10}|/|d_1| \sim 0.01$. The gravest four amplitudes were also found to differ by less than 10% if the number of modes N was chosen as 11 or 16, (see Table 2), and for the higher modes, the differences in the $|d_m|$ become larger but the amplitudes become smaller. The convergence and thus validity of these results seems reasonable. The convergence of the amplitudes of velocity $r_m|d_m|$ is slower with $r_{10}|d_{10}|/r_1|d_1| \approx 0.08$ to 0.2. The reflected Kelvin wave amplitude R in all cases examined is also close to that expected for the low frequency limit (2.23) where $R/I = -1.0$ and only the Kelvin waves contribute to coastal pressure.

The pressure fields $p(0^-, y)$ and $p(0^+, y)$ were then reconstructed and as shown in Fig. 2, the match in both the inviscid and frictional cases is excellent. The Collocation Method of course constrains the match to be exact at the $N + 1 = 12$ points where the difference equation for pressure (2.22) is evaluated. The results shown were however plotted using 40 points between $y = 0$ and $y = d$.

The results shown do differ substantially from those obtained where no Poincaré waves were included and exhibit a strong pressure gradient near $y = d$, with a corresponding jet $\tilde{U}(y)$ trapped to the Victorian coast, Fig. 3, where $\tilde{U} = \rho|f|dU/I$ denotes the nondimensional velocity. Observations of coastal sea level from the east Victorian coast (site 3; Fig. 1a) show that

TABLE 2. The magnitudes of the Poincaré wave amplitudes $|d_m|$ and R or T for the inviscid ($r = 0$) and frictional cases ($r \neq 0$). Each amplitude has been normalized by the incident wave amplitude I. Results are shown for the modes associated with CTW generation by a coastal flux and the scattering of a mode 1 CTW by a strait and a bay. Results for the case of a coastal flux with $N = 16$ Poincaré wave modes and $r \neq 0$ are also shown.

Poincaré mode	Coastal flux			Strait		Bay	
	$r = 0$	$r \neq 0$	$N = 16$	$r = 0$	$r \neq 0$	$r = 0$	$r \neq 0$
1	.9211	.7228	.7258	.3974	.3440	.5241	.4500
2	.4125	.2923	.2984	.1158	.1092	.1511	.1029
3	.2416	.1663	.1736	.0655	.0615	.1082	.0951
4	.1550	.1018	.1108	.0638	.0455	.0500	.0356
5	.1042	.0674	.0770	.0275	.0231	.0548	.0415
6	.0702	.0441	.0548	.0283	.0206	.0208	.0139
7	.0478	.0297	.0402	.0131	.0105	.0257	.0190
8	.0304	.0184	.0295	.0121	.0087	.0088	.0055
9	.0193	.0153	.0218	.0053	.0042	.0104	.0075
10	.0094	.0056	.0160	.0038	.0027	.0027	.0016
11	.0047	.0027	.0140	.0013	.0010	.0025	.0017
R	(−1.00, .052)	(−1.02, .054)	−(1.02, .06)	—	—	—	—
T	—	—	—	(1.27, .11)	(1.18, .30)	(.71, −.01)	(.68, −.06)

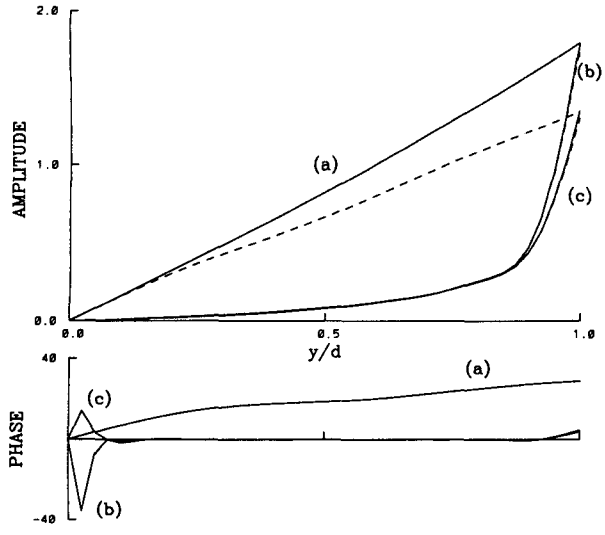

FIG. 2. The magnitude and phase difference of the pressure fields within the strait (2.9) (the solid curves), and on the shelf (2.19), (the dashed curves). Where no visible difference is apparent only the solid curve is shown. The three sets of curves were obtained using N Poincaré wave modes where for curves (a) $N = 0$, curves (b) $N = 11$ and $r = 0$ (an inviscid sea) and curves (c) $N = 11$ and $r \neq 0$ (a frictional sea). Note that pressure has been normalized by the incident Kelvin wave amplitude I.

$p(0^-, d) \approx 0.1\rho g$ Pa for a period of 240 h, (Middleton and Viera 1991). Since the Kelvin waves dominate coastal sea level, $p(0^-, d) \approx p_K(0^-, d) = I(e^{\alpha d} - e^{-\alpha d})$ so that $I \approx 0.06\rho g$ Pa. In this case the velocity of the jet trapped to the Victorian coast would be of order 47 cm s^{-1} and 31 cm s^{-1} in the inviscid and frictional cases, respectively. The existence of such a coastal-trapped jet follows from the fact that the velocity v is also implicitly matched in the region of the strait–shelf boundary; such a jet deflects to the east the northward excursion of water on the adjacent shelf that is driven by the CTWs. These results are illustrated in Fig. 4 where the pressure field normalized by I has been contoured for the eastern region of the strait. Note that the jet within the strait results in a shadow zone on the coast of the continental shelf.

The net energy flux (2.17) for each mode was also calculated at $y = d$ and scaled by the total flux that is directed through the eastern strait mouth, (2.11). The results (Table 3) show that modes 2 and 1 are dominant and indeed the flux magnitudes are similar to those found for the case where no Poincaré waves were allowed, $(\Gamma_1, \Gamma_2) = (0.18, 0.32)\Gamma_{st}$, and to those that may be obtained from (2.24) where U was assumed to be spatially uniform and $\Gamma_n/\Gamma_{st} \propto h_0 b_n^2$, (Table 1). Thus, to a first approximation, the energy flux carried by each mode might be estimated simply from the approximate expression (2.24). Such estimates would at least be useful in identifying the most energetic modes that might be generated by straits before further computation.

The similarity of the results obtained with and without the Poincaré waves also supports the contention by Middleton (1988) and Buchwald and Kachoyan

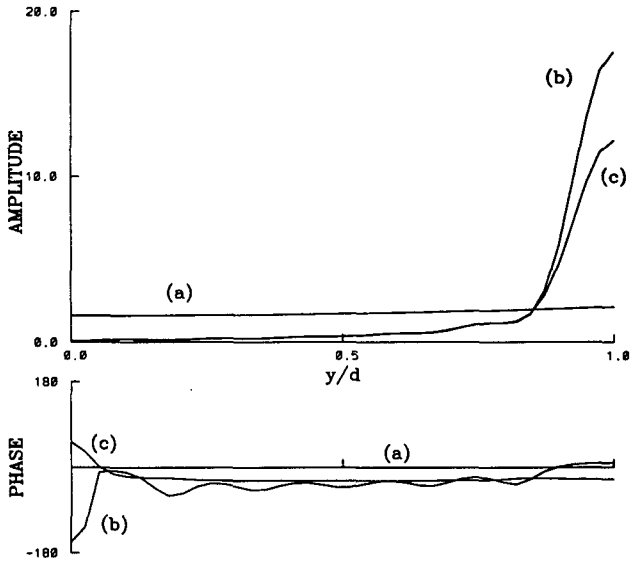

FIG. 3. The nondimensional magnitude and phase of the coastal flux velocity $\tilde{U} = \rho\,|f|\,dU/I$ obtained using N Poincaré wave modes where for curves (a) $N = 0$, curves (b) $N = 11$ and $r = 0$ and curves (c) $N = 11$ and $r \neq 0$.

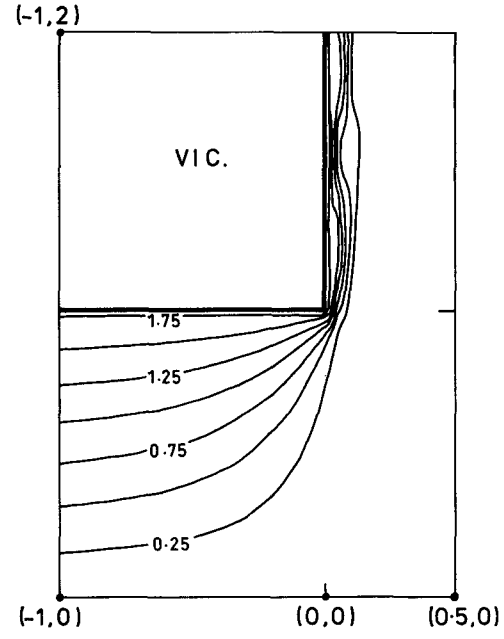

FIG. 4. The nondimensional amplitude of pressure (normalized by I) for the case of CTWs generated by an incident Kelvin wave (period 240 h) assuming $r = 0$ and $N = 11$ Poincaré wave modes. The geometry is as shown for Bass Strait in Fig. 1b and the (x, y) coordinate values shown have been scaled by d, the strait width. For the most energetic CTW modes 1 and 2 a quarter-wavelength is equal to $3.0d$ and $1.6d$, respectively.

TABLE 3. The percentage of net energy flux for the five dominant CTW modes and the totals of all CTW modes in the inviscid ($r = 0$) and frictional ($r \neq 0$) cases. Results are shown for the CTWs generated by a coastal flux and the scattering of a mode 1 CTW by a strait and a bay. The net flux Γ_{st} scattered into the strait and the bay is also shown.

	Coastal flux		Strait		Bay	
Mode	$r = 0$	$r \neq 0$	$r = 0$	$r \neq 0$	$r = 0$	$r \neq 0$
1	20.22	20.04	61.01	56.34	95.67	84.51
2	53.05	46.62	14.43	8.27	1.05	0.57
3	8.46	7.05	2.53	1.63	0.77	0.43
4	4.51	3.21	0.88	0.50	1.10	0.48
5	3.46	2.32	0.14	0.13	0.77	0.27
CTW total	98.67	84.89	79.85	67.37	99.99	86.58
Γ_{st}	—	—	20.13	19.58	0.00	0.10
Total	98.67	84.89	99.98	86.95	99.99	86.68

(1987) that the dominance of mode 2 found during the Australian Coastal Experiment results from its preferential generation by an oscillatory mass flux through Bass Strait. The inclusion of the Poincaré waves also leads to conservation of energy in the inviscid case, (Table 3), where the net flux of energy carried by all 11 CTW modes is 98.67% of that leaving the strait, Γ_{st}. With friction energy is no longer conserved and around 15% is dissipated in the region of the shelf between $y = 0$ and $y = d$. The flux of energy associated with each of the CTW modes 1 to 5 in Table 3 is also changed by less than 1% if the number of Poincaré wave modes is increased from 11 to 16. This stability again suggests that the results are reasonably convergent. In addition, the conservation of energy found in the inviscid case as well as the dominance of modes 2 and 1 suggests that the 11 CTW modes assumed are sufficient.

In the above we have not inquired into the origin of the incident Kelvin wave or the fate of the reflected wave. For Bass Strait, Middleton and Viera (1991) have shown that the incident wave may be the result of local wind forcing or remote forcing by CTWs that scatter energy into the western strait mouth. In either case the reflected wave (2.6) is subsequently backscattered at the western strait mouth, (Fig. 1b). The results here may be immediately generalized to incorporate this additional scattering, by splitting the incident wave amplitude I into two components I_0 and I_R where the former corresponds to say, a wave generated within the strait, and the latter to the wave that is reflected from the western strait mouth. The condition that pressure must vanish at the northwest strait corner implies that $p_R + p_{I_R} = 0$ which with (2.23) yields

$$I = I_0(1 + \beta^2 e^{-2il_0 L}), \tag{3.1}$$

where $\beta = \exp(-\alpha d)$. Thus with I_0 known, the (net) incident wave amplitude I may be determined. (Note that for Bass Strait $|\beta^2 e^{-2il_0 L}| \approx 0.22$.)

We may also consider the case where the strait is connected to a large enclosed sea such as Hudson Bay. Wright et al. (1987) have shown that atmospheric pressure variations over that bay can lead to an oscillatory flux through Hudson Strait with a corresponding sea-level signal $\hat{\eta}$ [their Eq. (14)] at $\mathbf{x} = (0, d)$ for our geometry. The analysis here is again applicable since by equating the Kelvin wave pressure field within Hudson Strait to $\rho g\hat{\eta}$ we obtain an incident wave amplitude of

$$I = \beta\rho\hat{\eta}/(1 - \beta^2). \tag{3.2}$$

The bathymetry of Hudson Strait and the adjacent shelf does differ considerably from that of the Bass Strait region and in particular $(b_0, b_1, b_2) = (1.7, 4.0, 1.5) \times 10^{-3}$ cm$^{-1/2}$ so that mode 1 may be expected to be dominant, (Middleton and Wright 1991).

4. Scattering into a strait or bay

Here we consider the problem of how an incident CTW p_I shown in Fig. 5 may scatter energy into a strait or bay. We address the strait problem first and formulate the solution for $x \leq 0$ as

$$p(x, y) = Te^{-(\alpha y - il_0 x)} + Re^{\alpha y - il_0 x} + \sum_1^\infty d_m \sin(r_m y + \epsilon)e^{r_m x}, \tag{4.1}$$

where T and R now denote the amplitudes of Kelvin waves (driven by the incident CTW) and the latter wave is included so as to follow for possible reflection at $x = -L$, the eastern strait mouth. Note that we assume that the Poincaré wave field that is trapped at the eastern strait mouth ($x = -L$) may be ignored at the western mouth. For Bass Strait, $L \approx 416$ km and the Poincaré wave fields decay by more than $e^{-\pi L/d} \approx 0.003$ over the length of the strait. In addition, we have also seen that the reflected Kelvin wave amplitude may be reasonably determined by ignoring the Poincaré wave field and using the condition (here) that pressure vanishes at $\mathbf{x} = (-L, d)$. In this case (4.1) implies

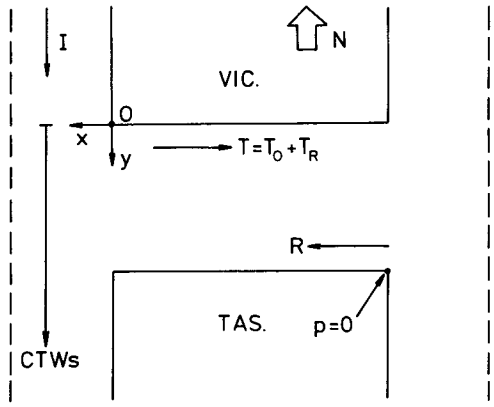

FIG. 5. A schematic illustration showing the idealized geometry for the scattering of an incident CTW (I) into transmitted (T) and reflected (R) Kelvin waves. The sense of CTW propagation is indicated. Note that the transmitted wave may be regarded as consisting of two components T_0 and T_R which respectively correspond to a wave that is driven by the incident CTW field and a wave that results from the scattering of the reflected wave by the western strait mouth.

$$R = -\beta^2 T e^{-2il_0 L}, \tag{4.2a}$$

where $\beta = \exp(-\alpha d)$.

For a blocked strait or bay, the solution is again formulated as (4.1) and the reflection coefficient may also be determined if the Poincaré wave contribution to coastal pressure is ignored. In this case, since there can be no flow through the bay at $x = -L$, the Kelvin wave pressure at $\mathbf{x} = (-L, 0)$ and $\mathbf{x} = (-L, d)$ must be equal and from (4.1) we then obtain

$$R = \beta T e^{-2il_0 L}. \tag{4.2b}$$

In the inviscid limit there is no net flux of energy into the bay. In addition, if the phase lag $2l_0L$ may be ignored, and $|2l_0L| \approx 0.2$ for Bass Strait at a period of 240 h, then the instantaneous net mass flux into the bay is also zero.

Now, on the western shelf we assume that pressure is determined by the incident wave $p_I(0^+, y) = I\exp(iK_I y)$ and by the CTWs generated by the Kelvin and Poincaré wave fields within the strait as described in the previous section. Thus, we have

$$p(0^+, y) = p_I(0^+, y) - \rho f \int_0^y U(y)G(\zeta - y)d\zeta, \tag{4.3}$$

where

$$-\rho f U(\zeta) = \alpha(Re^{\alpha y} - Te^{-\alpha y}) + \sum_1^\infty d_m r_m \cos(r_m y). \tag{4.4}$$

The unknown T, R and d_m are again to be determined by matching the CTW pressure (4.4) to that within the strait (4.1). At low frequencies where $\epsilon \approx 0$, the amplitudes T and R may be immediately estimated since the CTW coastal pressure at $y = 0$ is given by $p_I(0^+, 0) = I$ and must be equal to that of the Kelvin waves, $p_K(0^-, 0) = T + R$ so that

$$T = I/(1 - \beta^2 e^{-2il_0 L}) \tag{4.5a}$$

and is given by $T = (1.24 + 0.007i)I$ in the inviscid case. (In this case the imaginary component of T arises from the phase lag of the wave that is reflected by the eastern shelf.) It is worth noting that the transmitted wave may be split into two components of amplitude T_0 and T_R which respectively correspond to a wave that is driven by the incident CTW field, in that coastal pressure is equated and $T_0 = I$, and a component of the reflected wave that is backscattered by the western strait mouth such that at the northwest corner $p_R + p_{T_R} = 0$ and $T_R = -R$. This formulation, used by Middleton and Viera (1991), is equivalent to that used here and consistent with (4.2a) and (4.5a).

For the case of a bay, equating the incident CTW and Kelvin wave pressure fields at the northwest corner results in

$$T = I/(1 + \beta e^{-2il_0 L}) \tag{4.5b}$$

and in the inviscid case is given by $T = (0.69 - 0.05i)I$.

More generally, T, R and d_m are to be obtained by matching pressure across the strait mouth. The solution technique is as before, and the following results were obtained assuming the 11 gravest CTW modes, the geometry of Bass Strait and a period of 240 h.

a. Results for Bass Strait

The Poincaré wave amplitudes shown in Table 2 were determined assuming a mode 1 incident CTW and again show a rapid decrease with mode number in both the inviscid and frictional cases. The coefficient of the transmitted Kelvin wave is determined as $T \approx (1.27 + 0.11i)I$ in the inviscid case and close to that given by (4.5a) which follows from equating the pressure of incident CTW and transmitted Kelvin waves at $\mathbf{x} = 0$. The match for pressure in both the inviscid and frictional cases is again very good (Fig. 6) and jets trapped to both the Victorian and Tasmanian coasts are now found, (Fig. 7). To estimate the magnitudes of these jets we note that Middleton and Viera (1991) have identified sea-level variations of ±0.1 m at Portland (Fig. 1a) on the west Victorian coast. If we assume these variations to be due to a mode 1 CTW, then $I \approx 0.1\rho g$ Pa and the dimensional amplitudes at the Victorian and Tasmanian coasts are of order 13 cm s^{-1} and 26 cm s^{-1}, respectively, with the latter lagging the former by 65° or so. The magnitudes of these coastal jets are in crude agreement with the velocity data obtained from sites 10 and 7 (Fig. 1a), although the agreement may be fortuitous since we have here made no allowance for the effects of King Island. In addition, there is as yet no data to support the as-

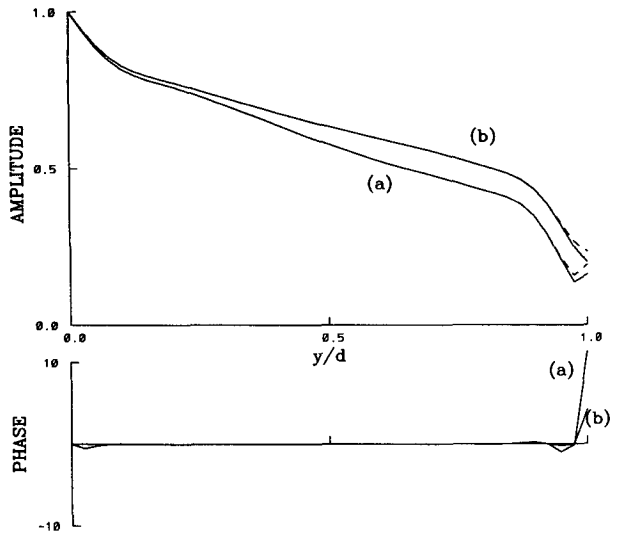

FIG. 6. The magnitude and phase difference of the pressure fields within the strait (4.1) (solid curves) and on the shelf (4.3) (dashed curves) for the scattering of a mode 1 CTW incident on a strait. Pressure has been normalized by I the incident wave amplitude. Eleven Poincaré wave modes were assumed and curves (a) and (b) pertain to the inviscid ($r = 0$) and frictional ($r \neq 0$) cases.

sumption that sea-level variations at Portland are indeed due to a mode 1 CTW.

Returning to the idealized calculations we note that the total flux of energy in the inviscid case is conserved to within 0.02% (Table 3) with modes 1 and 2 accounting for 61% and 14% of that passing $y = d$, (Tasmania). In the frictional case 13% of the incident wave energy is dissipated between $y = 0$ and $y = d$ on the shelf. In both cases however, nearly 20% of the incident

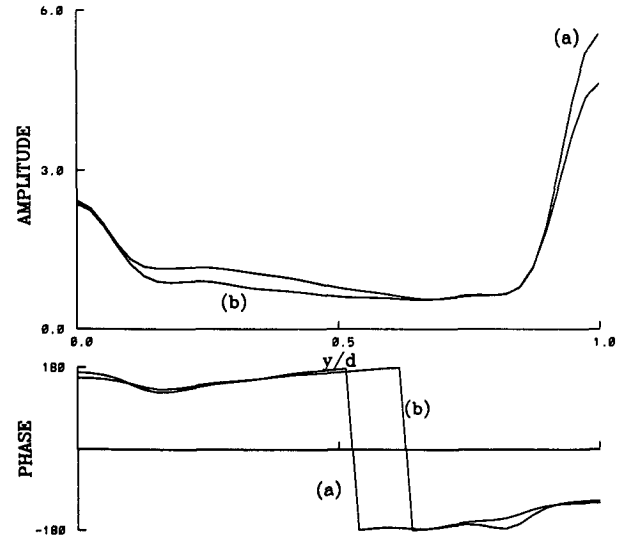

FIG. 7. As in Fig. 6 but for the magnitude and phase of the nondimensional velocity $\tilde{U} = \rho |f| dU/I$.

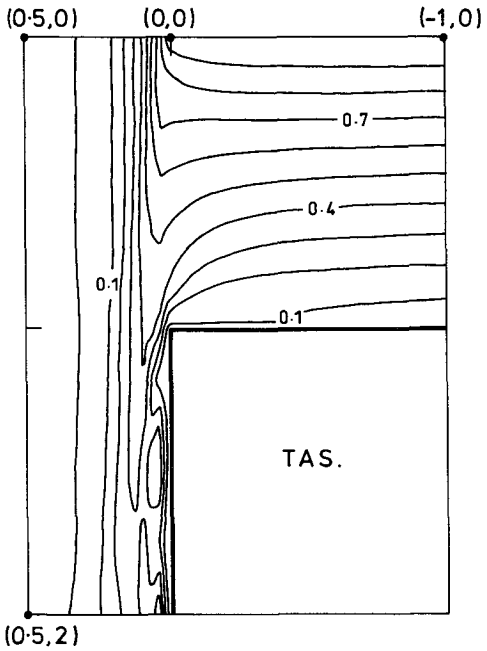

FIG. 8. The nondimensional amplitude of pressure (normalized by I) for the scattering of a mode 1 CTW incident on the western mouth of Bass Strait assuming $r = 0$ and $N = 11$ Poincaré wave modes. A period of 240 h was assumed and the (x, y) coordinate values shown have been scaled by d the strait width. For the most energetic CTW modes 1 and 2 a quarter-wavelength is given by $3.0d$ and $1.6d$, respectively.

CTW energy enters the strait. The results for the inviscid sea are also illustrated in Fig. 8 where the amplitude of the pressure field normalized by I, has been contoured for the western region of Bass Strait.

The dependency on frequency of the energy flux carried by each CTW mode at $y = d$ has also been determined. In the inviscid limit, the net flux for mode 1 decreases with increasing frequency (Fig. 9a) with a corresponding increase in the flux carried by mode 2: more than 50% of the incident energy remains in mode 1. The total flux carried by all other CTW modes is small, while around 20% of the incident energy is scattered into the strait. With friction (Fig. 9b), the results are similar except that the flux carried by modes 1 and 2 are reduced with the remaining 13% of the incident energy now being dissipated on the shelf.

As noted earlier, the long-wave approximation assumed is formally invalid for periods shorter than 10 days (240 h) so that the results presented for shorter periods are at best only qualitatively correct.

Results for an incident mode 2 wave were also obtained and as shown in Fig. 10, around 50% of the net flux is now scattered into the strait as compared to 20% for a mode 1 incident wave. To understand this result we note that for a mode n incident CTW, the net flux at $y = 0$ is from (2.17) given by

$$\Gamma_I = -I^2/(4\rho f b_I^2) \qquad (4.6)$$

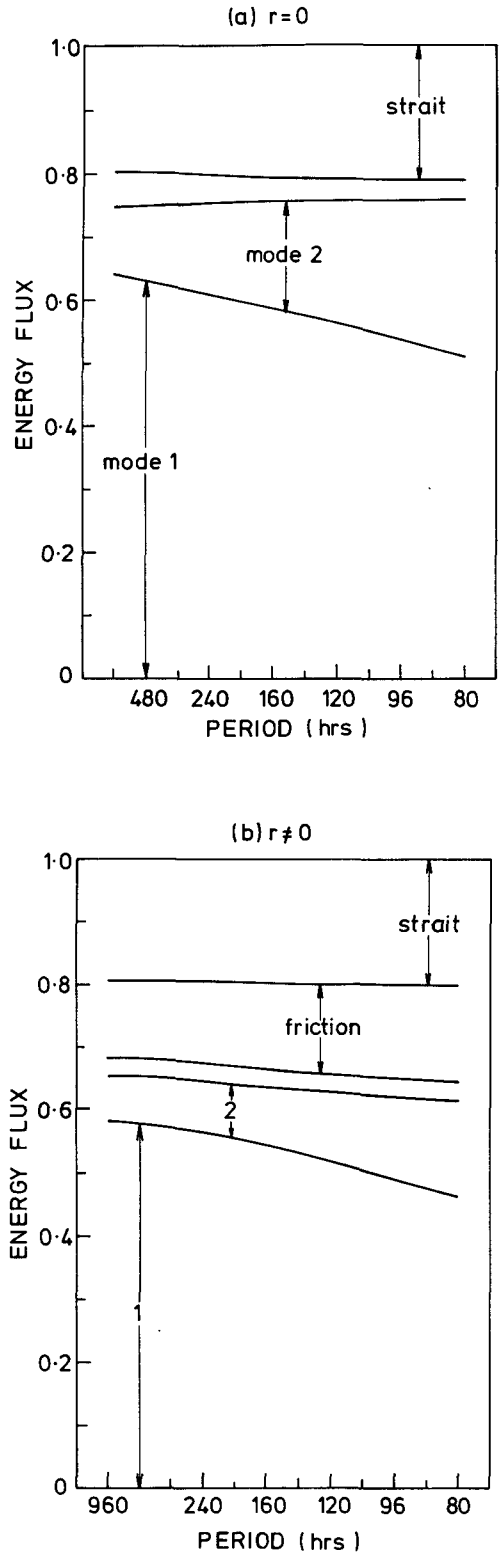

FIG. 9. The fractions of net energy flux that is scattered into the strait and into modes 1 and 2 at $y = d$ for a mode 1 incident CTW. (a) and (b) correspond to the inviscid ($r = 0$) and frictional cases ($r \neq 0$), respectively.

for $p_I = Ie^{iK_I y}$. Neglecting the phase lag of Kelvin wave propagation within the strait also implies that (4.2) reduces to $R = -\beta^2 T$ and since $p(-L, d)$ is zero, pressure all along the Tasmanian coast must vanish and $p(0, d) = 0$. In this case the net flux into the strait (2.11) simplifies to

$$\Gamma_{st} = (h_0/4\rho f)p_K(0, 0)p_K^*(0, 0), \qquad (4.7)$$

and if the coastal Poincaré wave pressure field can be ignored, then $p_K(0, 0) = p_I(0, 0)$ so that

$$\Gamma_{st} = (h_0/4\rho f)p_I(0, 0)p_I^*(0, 0).$$

In this form it is apparent that the net flux into the strait depends principally on the coastal pressure of the incident CTW field. Since $I = p_I(0, 0)$, the result may also be rewritten as

$$\Gamma_{st} = -h_0 b_I^2 \Gamma_I. \qquad (4.8)$$

For a mode 1 incident wave $h_0 b_1^2 = 0.195$ (Table 1) while for a mode 2 wave $h_0 b_2^2 = 0.503$ where both estimates of Γ_{st} are very close to those obtained in the more general analysis; see Figs. 9 and 10.

The scattering of an incident Kelvin wave (mode 0) was also investigated and only 1.3% of the flux was found to be scattered into the strait and 1.3% into other modes. The amount scattered into the strait was again, to a good approximation, given by (4.8). While only a small fraction of the incident Kelvin wave energy is scattered, it should be noted that again, a jet was found trapped to the Tasmanian coast, which is qualitatively similar to that for a mode 1 incident CTW, (see Fig. 7). That little of the Kelvin wave energy is scattered is a consequence of the fact that most of the energy flux of this wave is carried in deep water far from the strait.

This result and those for CTWs 1 and 2 show that the scattering of energy away from the incident mode becomes more severe at higher mode number and frequency and thus also for larger values of $k_I d$. Such a result might be expected since as the longshore scale of the wave approaches the strait width d the scattering should become more severe. As we have seen, the amount scattered into the strait may be estimated from (4.8). A similar simple rule for the scattering of energy among the CTW modes does not seem evident.

b. Results for a bay

Finally, the scattering by a rectangular bay was also investigated using the reflection coefficient (4.2b) and the parameters for the strait. In the inviscid limit, the net energy flux into the bay is zero although the Poincaré and Kelvin wave fields set up can act to scatter energy of the incident wave.

The Poincaré wave amplitudes for an incident mode 1 CTW at the 240 h period were determined (Table 2) and those for the dominant four gravest modes were

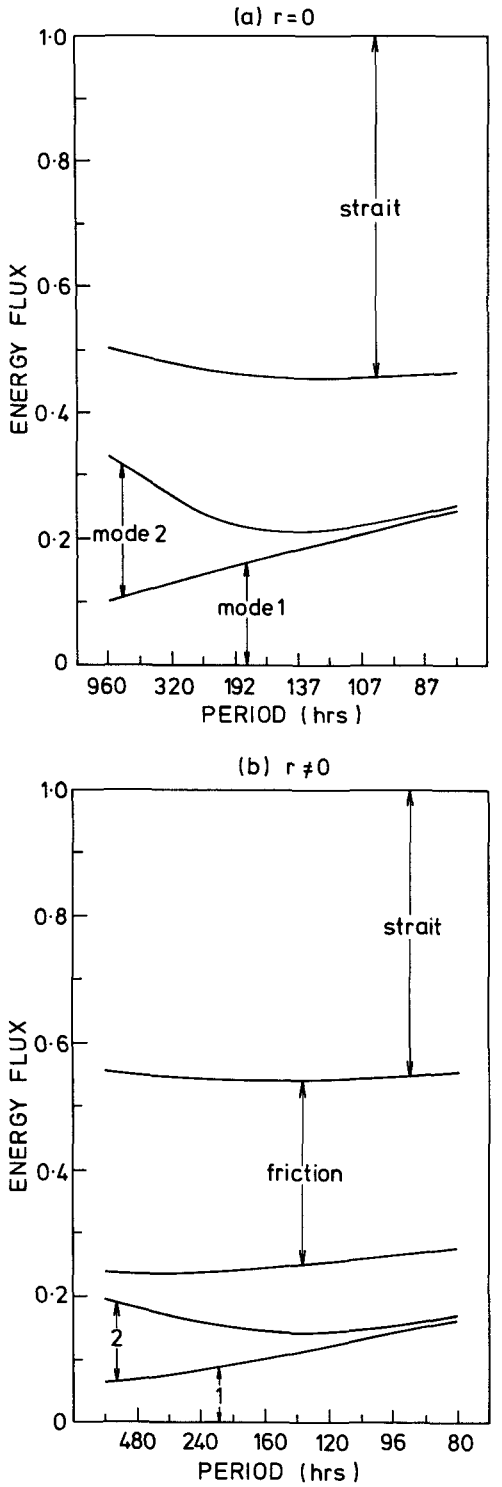

FIG. 10. As in Fig. 9 but for a mode 2 CTW incident on the strait.

found to vary by less than 5% if $N = 16$ or $N = 11$ modes were chosen; the fifth mode varied by 15%. For the inviscid case, the transmission coefficient in Table 2 is also very close to that expected if the incident CTW and Kelvin wave pressure fields may be assumed to match exactly where from (4.5b) $T \approx (0.69 - 0.05i)I$.

The match for pressure in both the inviscid and frictional cases (Fig. 11) is again very good and jets trapped to both coasts at $y = 0$ and $y = d$ are apparent (Fig. 12), and around 180° degrees out of phase. The net mass flux into the bay is also close to zero since at low frequencies u is geostrophic and pressure at the coast is determined by the Kelvin waves. Results for the net energy flux (Table 3) show that most energy remains in the mode 1 incident wave although in the frictional case about 13% is dissipated on the shelf between $y = 0$ and $y = d$.

The dependence of the scattering on frequency and bay width was also determined for the inviscid case and as shown in Fig. 13, wider bays or higher frequencies imply an increase in the scattering of energy of the incident first mode amongst the other CTW modes. The mode 1 flux is also shown for several values of $k_1 d$ and, as is apparent, the scattering of energy into other modes increases as the incident wavelength decreases. The net flux carried by mode 1 past $y = d$ is dependent both on $k_1 d$ and frequency so that again no simple rule for the scattering of the incident CTW is evident.

5. Summary and discussion

The low frequency scattering of long CTWs both into and out of straits has been examined by extension of the analysis of Middleton (1988) for the generation of CTWs by a coastal flux. In that work, a prescribed oscillatory flux $U(y)e^{-i\omega t}$ through a strait was shown

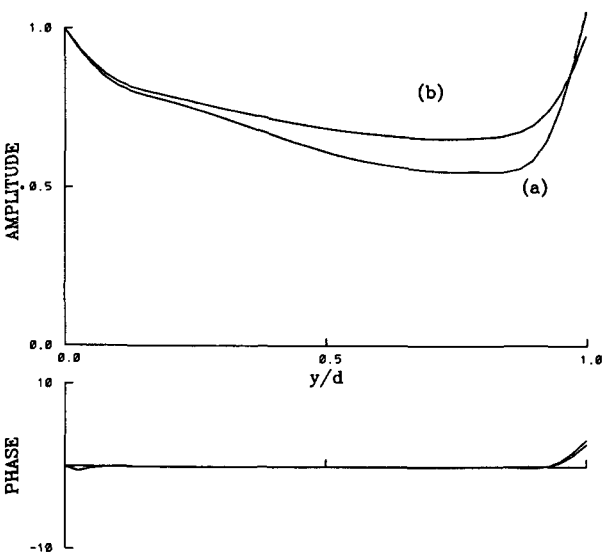

FIG. 11. The magnitude and phase difference of the pressure fields within the strait (solid curves) and on the shelf (dashed curves) for the scattering of a mode 1 CTW incident on a bay. Curves (a) and (b) pertain to the inviscid ($r = 0$) and frictional ($r \neq 0$) cases.

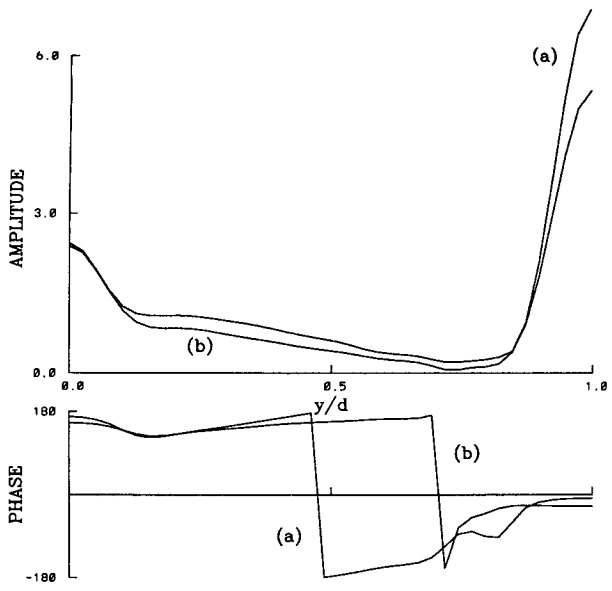

FIG. 12. As in Fig. 11 but for the magnitude and phase of the nondimensional velocity $\tilde{U} = \rho\,|f|\,dU/I$.

to be analogous to forcing by wind stress so that a simple forced wave equation was obtained for each CTW mode generated. Here the velocity flux $U(y)$ and its associated pressure field were not prescribed, but rather expanded in terms of Kelvin wave and Poincaré wave modes, the amplitude of which were determined through the requirement that pressure be continuous across the strait–shelf boundary. A Collocation Method was used where the number of Poincaré (and CTW) modes was assumed finite and pressure was evaluated at sufficient points to determine all unknown amplitudes.

For the case of CTWs generated by a coastal flux, specific results were obtained for a Kelvin wave incident on the eastern mouth of Bass Strait, at a period of 240 h, the energy containing band, (Middleton and Viera 1991). Out of the 11 Poincaré wave modes assumed in the analysis, the gravest four were found to be dominant, resulting in a jet that is trapped to the Victorian coast and of amplitude $U(d) \sim 31$ cm s^{-1} for an incident Kelvin wave amplitude I of $0.06\rho g$ Pa, (Middleton and Viera 1991). The jet is a manifestation of the match for velocity and acts to drive northward excursions of fluid on the shelf away from the east Victorian coast so that the northward component of velocity v is locally zero and thus matches that on the Victorian coast where $v \equiv 0$.

The jet $U(y)$ also acts to generate CTWs on the shelf, and of the net energy flux leaving the strait Γ_{st}, around 20% and 50% was found to be carried by the CTW modes 1 and 2, respectively. These results are qualitatively similar to those predicted in the absence of the Poincaré wave field where for the nth CTW mode, the flux is approximately given by

$$\Gamma_n/\Gamma_{st} \approx h_0 b_n^2 \operatorname{sinc}^2(k_n d/2). \qquad (5.1)$$

However, without the Poincaré waves pressure is not continuous, and the total flux of energy given by (5.1) is not conserved: $\Gamma/\Gamma_{st} \approx 0.78$. The inclusion of these modes here results in an excellent match for pressure with energy nearly conserved: $\Gamma/\Gamma_{st} \approx 0.98$. The validity of these results was also supported by the convergence of the Poincaré modal amplitudes where for pressure, the amplitudes decayed rapidly with $d_{10}/d_1 \approx 0.01$. In addition, the flux of energy was dominated by contributions from modes 1 and 2 suggesting that the total of 11 CTW modes assumed was adequate.

The problem of how CTW energy may be scattered into a strait or a bay was also addressed. Pressure on the shelf was assumed to consist of that due to the incident wave p_I as well as the CTWs generated by the velocity flux $U(y)e^{-i\omega t}$ that arises at the shelf–strait

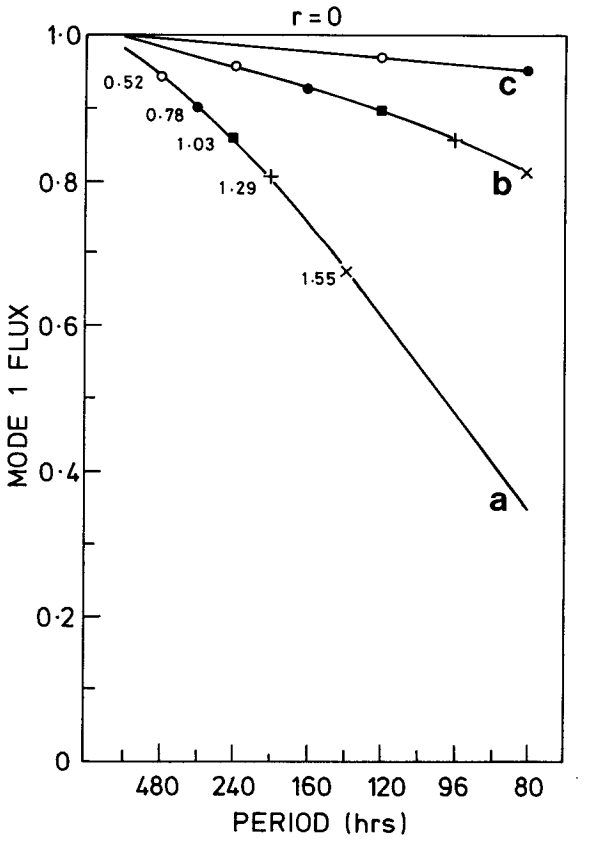

FIG. 13. The fraction of net energy flux in the mode 1 CTW after scattering by a bay. Curves (a), (b) and (c) were obtained for a bay of width d equal to $2d_0$, d_0 and $d_0/2$ where $d_0 = 230$ km and $r = 0$. The values next to the points indicated denote values of $k_1 d$ and show the severity of scattering as a function of the ratio of bay width to the wavelength of the incident CTW mode.

boundary. Within the strait or bay a scattered Kelvin and Poincaré wave field was again assumed. At very low frequencies where $\epsilon \sim |\omega/f| \ll 1$, the fraction of net energy scattered into the strait was given by

$$\Gamma_{st}/\Gamma_I = -h_0 b_I^2, \qquad (5.2)$$

where Γ_I denotes the net flux of the mode I incident wave. This result and the approximate expression (5.1) both underline the importance of the coupling coefficients b_n in determining the importance of straits in wave scattering and generation.

For the case of Bass Strait, the result (5.2) was also shown to be reasonably valid at higher frequencies where ϵ is not negligible through the inclusion of the Poincaré wave modes in the match for pressure. Indeed, for the incident CTW modes 0, 1 and 2, the respective percentage of energy scattered into the strait was estimated at around 1.3%, 20%, and 50% and close to that given by (5.2). Of the energy propagating past the strait, the percentage associated with the incident wave decreases with increasing mode number. For modes 0, 1 and 2 the flux is reduced to 97.6%, 61% and 10% of the incident wave so that mode 2 is most severely scattered. An increase in scattering was also found to occur at higher frequencies, and in both cases the scale of the incident wave becomes smaller compared to the strait width. However, no simple rule seems apparent for the net flux carried by the scattered CTW modes.

In all cases examined, the scattering of CTW energy into the strait resulted in jets $U(y)$ trapped to both coasts that bound the strait. For the western region of Bass Strait, velocity variations of order 25 cm s^{-1} have been observed near the Tasmanian coast, which are consistent with an assumed mode 1 incident CTW and the observed coastal pressure variations of $0.1\rho g$ Pa at a period of 240 h, (Middleton and Viera 1991). The agreement here is perhaps fortuitous since the idealized bathymetry assumed here makes no allowance for features such as King Island, (Fig. 1a), which will act to modify the Poincaré wave field determined here. Note that the Kelvin wave field *within* the strait is not effected by features such as King Island since energy is almost completely transmitted past such obstacles, (Middleton and Viera 1991).

The problem of how CTWs may be scattered into western mouth of Bass Strait has also been examined by Clarke (1987). In that analysis, a mode 1 incident CTW was assumed to propagate past the strait as an escarpment wave, the pressure field of which was determined using a semi-infinite model for the strait itself. The transmitted Kelvin wave and Poincaré wave fields were not included in the analysis however, and indeed the latter are excluded from his analysis since the model strait assumed was of a semi-infinite width. Using the escarpment wave pressure at $x = (-L, 0)$ Clarke estimated that the net flux entering the strait should be about 7% of the incident mode 1 wave. As shown here and by Middleton and Viera (1991), the net flux into the strait is around 20% of an incident mode 1 CTW, and the result is simply obtained by equating coastal pressure with that of the Kelvin wave field within the strait. The escarpment wave analysis of Clarke (1987), while interesting in its own right, is perhaps not appropriate to the scattering of CTW energy into Bass Strait.

In the analysis here results were also obtained for the scattering of incident CTW energy by a flat rectangular bay. In the inviscid limit, the net energy flux into the bay is zero although the Poincaré and Kelvin wave fields can act to scatter incident energy among the other CTW modes. Coastal jets $U(y)$ were again found on either side of the bay with a phase lag of around 180° that might be expected at very low frequencies, since the net flux of mass into the bay must vanish. The scattering of the incident wave was also found to increase with both frequency and bay width although no simple rule for the energy transferred between modes was evident. A final result worth noting follows from the fact that within the bay, coastal pressure will vary little since it is determined by the large-scale Kelvin wave field, and will also be equal to that on the immediate adjacent shelf. These results perhaps explain why tide-gauge data from within bays can be a good indicator of CTW activity on adjacent shelves.

The applicability of the above solution technique and results is of course restricted by the long-wave assumption where $(\omega/f)^2$ is required to be small and the generated CTWs nondispersive. The latter condition need only pertain to those dominant energy containing CTWs and can readily be checked by calculating the modes both with and without the longwave approximation, (see Brink and Chapman 1985). The long-wave approximation can be relaxed by inclusion of Poincaré wave modes in the barotropic, subinertial analysis of Buchwald and Kachoyan (1987) so as to make pressure everywhere continuous, (Buchwald, personal communication). However, in this analysis the rigid-lid approximation and an idealized exponential shelf topography is assumed.

A further restriction on the analysis here is that the width d of the strait or bay should be less than or equal to the deformation radius of the strait since the approximate form of the Poincaré waves used here is then only valid. For specific applications the effects of stratification should also be included as outlined, as well as a more realistic model for friction on the shelf. The results are perhaps most severely restricted by the idealized bathymetry chosen. For example, we have implicitly assumed that the shelf depth at the coast is equal to that of the strait h_0 and thus have not had to enquire into how incident or generated CTWs might be scattered as they enter or leave the region of the strait (see Middleton and Wright 1991). In addition no allowance has been made for bays or straits of vari-

able width or depth. However, the solution technique is relatively simple and should prove useful in furthering our understanding of the scattering of CTWs in and out of straits and bays.

Acknowledgments. I thank Ted Johnson for a useful discussion as well as Fernando Viera for preparing some figures. This work was supported by the Australian Research Council, Grant A48830274.

REFERENCES

Brown, P. J., 1973: Kelvin-wave reflection in a semi-infinite canal. *J. Mar. Res.*, **31,** 1–10.

Brink, K. H., 1982: The effect of bottom friction on low-frequency coastal trapped waves. *J. Phys. Oceanogr.*, **8,** 919–922.

——, and D. C. Chapman, 1985: Programs for computing properties of coastal-trapped waves and wind-forced motions over the continental shelf and slope. Wood Hole Oceanogr. Inst., Tech. Rep. WHOI-85-17, 99 pp.

Buchwald, V. T., and B. J. Kachoyan, 1987: Shelf waves generated by a coastal flux. *Aust. J. Mar. Freshwater Res.*, **38,** 429–37.

Chapman, D. C., 1983: On the influence of stratification and continental shelf and slope topography on the dispersion of subinertial coastally trapped waves. *J. Phys. Oceanogr.*, **13,** 1641–1652.

Church, J. A., and H. J. Freeland, 1987: The energy source for the coastal-trapped waves in the Australian Coastal Experiment Region. *J. Phys. Oceanogr.*, **17,** 289–300.

——, and R. L. Smith, 1986: Coastal-trapped waves on the east Australian continental shelf. Part I: Propagation of Modes. *J. Phys. Oceanogr.*, **16,** 1929–1943.

Clarke, A. J., 1987: The origin of the Australian Coastal Experiment coastally trapped waves. *J. Phys. Oceanogr.*, **17,** 1847–1859.

——, and S. Van Gorder, 1986: A method for estimating wind-driven frictional, time-dependent, stratified shelf and slope water flow. *J. Phys. Oceanogr.*, **16,** 1011–1026.

Middleton, J. F., 1988: Long shelf waves generated by a coastal flux. *J. Geophys. Res.*, **93**(C9), 10 724–10 730.

——, and D. G. Wright, 1991: Coastal-trapped waves on the Labrador Shelf. *J. Geophys. Res.*, in press.

——, and F. Viera, 1991: The forcing of low frequency motions within Bass Strait. *J. Phys. Oceanogr.*, **21,** 695–708.

Stocker, T. F., and E. R. Johnson, 1989: Topographic waves in open domains. Part II: Bay modes and resonances. *J. Fluid Mech.*, **200,** 77–93.

Webster, I., and S. Narayanan, 1988: Low-frequency current variability on the Labrador Shelf. *J. Geophys. Res.*, **93**(C7), 8163–8173.

Wright, D. G., D. A. Greenberg and F. G. Majaess, 1987: The influence of bays on adjusted sea-level lower adjacent shelves with application to the Labrador Shelf. *J. Geophys. Res.*, **92**(C13), 14 610–14 620.